CHARACTERIZATION AND AGEING OF MEDIEVAL-LIKE GLASS FOR THE DESIGN OF PROTECTIVE COATINGS

LAVINIA DE FERRI

Dipartimento di Scienze della Terra, Università di Modena e Reggio Emilia, Largo S. Eufemia 19, 41100 Modena, Italy

ABSTRACT

Glass, compositionally similar to that of the medieval stained glass windows, was produced and characterized through a multi-technique approach to investigate the structural modifications induced by different amounts of potassium as flux, and their influence on the glass alteration processes.

Ageing experiments were performed simulating separately the two mechanisms responsible for the glass alteration: leaching and dissolution. A clear relationship between the glass K-content and the degree of de-polymerization of the silicate network was found through XRPD, FT-IR, and Raman spectroscopy analyses. Moreover the ageing experiments showed a correlation between the glass K-content and the alteration degree; in particular, it was observed that the most K-rich and depolymerized samples were also the most alterable.

These structural studies were aimed to the design of water repellent protective coatings, matching the requirements of the Conservation of Cultural Heritage. Some hybrid sol-gel coatings, based on TEOS (Tetra-ethyl-orto-silicate), that guaranties the chemical and physical compatibility with the glass, and the organically functionalized Si-alkoxides, were prepared and characterized to obtain a good water repellency. Their performance was tested through accelerated ageing under UV-light and exposure to SO_2-saturated atmosphere.

INTRODUCTION

The glass chemical stability depends on both the glass chemistry (*i.e.*, the relationship between formers, modifiers and stabilizers) and the environmental parameters, especially the presence of water on glass surface and its *p*H. Historical stained glass windows are in permanent contact with water in form of rain, fog, snow, or humidity whose condensation generally can take place also on the glass internal side.

These phenomena are particularly dangerous for the potash-lime-silica glass (PLS), produced in the central Europe since ~ 800 A.D. and mostly used for cathedrals windows, since potassium ions can very easily be leached and consequently a very strong dissociated base, leading to the dissolution of the glass network, forms in the liquid medium.

The attention paid to the conservation of these historical windows lead to the development of several protection methods, but only in the last decades the application of hybrid materials allows to fulfill the requirements of the Conservation of Cultural Heritage as the transparency, chemical and thermal stability and the compatibility with the substrate.

GLASS PRODUCTION AND CHARACTERIZATION

Three recipes (V1, V2, and V3), containing increasing amounts of K_2O as fluxing agent and chosen on the basis of archaeometric studies (Sterpenich & Libourel, 2001; Schalm *et al*., 2007, 2010), were used to prepare glass samples mimicking the medieval glass chemistry (de Ferri *et al.*, 2012). The sample compositions are reported in Table 1.

The glass samples were characterized by XRPD (CuKα radiation; λ = 1.54056 Å) using a Thermo Scientific ARL X'tra powder diffractometer equipped with a Thermo Electron solid state detector. The patterns were collected between 5 and 90° 2θ, with 0.02° 2θ steps and counting time of 2 s/step. The patterns showed the shift of the broad diffraction maximum toward higher 2θ angles, with respect to the silica-glass (21-22° 2θ), with increasing the K_2O amount.

Table. 1 - XRF chemical analysis of the reproduced glass varieties V1, V2 and V3 (oxide wt.%).
The measurement accuracy is lower than 3%.

	SiO_2	CaO	MgO	K_2O	P_2O_5	Na_2O	Al_2O_3	TiO_2
V1	61.11	18.50	3.82	12.29	1.67	0.38	1.99	0.09
V2	57.07	18.64	3.57	16.74	1.62	0.67	1.38	0.06
V3	53.10	17.53	3.24	23.49	1.52	0.26	0.73	0.03

The diffraction maximum position varies from 28 to 29.5° 2θ passing from V1 to V3: it is commonly assumed (Göttlicher & Penthigaus, 1996; Swenson & Böriesson, 1998; Mukai *et al.*, 2007) that the main band of the XRPD pattern of a silicate glass contains information regarding the medium-range order (MRO) and even if the exact relationship between the band position and the MRO is still widely discussed in literature, the observed 2θ increase with the glass K-content can be reasonably related to the network de-polymerization (Du & Corrales, 2006).

The vibrational properties of the glass were investigated by μ-FT-IR spectroscopy employing a Nicolet Nexus spectrophotometer, equipped with a Thermo Nicolet Continuμm™ microscope, in μATR (Attenuated Total Reflectance) mode, using a diamond crystal. Spectra were collected in 120 accumulation cycles in the 600-4000 cm^{-1} spectral range, with ~ 4 cm^{-1} resolution. Raman spectra were acquired with the 488 nm line of an Argon laser (~ 25 mW power), using a Jobin-Yvon HR 800 LabRam Spectrometer equipped with and Olympus microscope, in the spectral range 150-1500 cm^{-1}, with ~ 2 cm^{-1} resolution. Each spectrum was elaborated subtracting the background with the LabSpec® software using linear segments (Colomban *et al.*, 2006); a routine method developed at the LADIR laboratory (Colomban *et al.*, 2006) was implemented with the Origin® peak-fitting software for the Gaussian de-composition of the stretching band into the different vibrational contributions, on the basis of the Q^n model (n expresses the number of bonding oxygens -BO- per Si-centered Q tetrahedron) (Colomban *et al.*, 2006).

Consistently with the amount of flux introduced into the glass (Abo-Naf *et al.*, 2002), the decomposition performed on the FT-IR spectra shows the red-shift of the three main bands (Fig. 1a). The first at about 750 cm^{-1} controversially attributed to the Si-O-Si bending or symmetric stretching, that centered at about 900-950 cm^{-1} due to the $Si-O^-K^+$ stretching vibrations and the last one at about 1050-1100 cm^{-1} given by the Si-O-Si anti-symmetric stretching, normally found at higher wavenumbers in pure silica glass (Torres *et al.*, 2008).

This effect is related to the lengthening, and so to the weakening, of the Si-O bonds. The band shift is attributed to the decrease of restrictions in the system: the addition of alkaline cations reduces the degree of connectivity of the three-dimensional network since the number of non-bridging- oxygens (NBO) increases.

The Raman spectra of silicate glasses are characterized by two main bands due to the bending (centered at ~ 500-600 cm^{-1}) and stretching (centered at ~ 1000-1100 cm^{-1}) motions. The spectra were studied by decomposing the stretching band (between 750 and 1250 cm^{-1}) into the Q^n structural units (Fig. 2), and detecting the position of the two spectra maxima: the bending band maximum (δ_{max}) and the stretching band maximum (ν_{max}). The polymerization index I_p, defined as the ratio between the areas of the bending and of the stretching bands (Colomban, 2003), was calculated.

Q^n speciation

The short-range structure of the silicate glass can be described in terms of Q^n configurations, each one originating a specific Raman signal convoluted in the Raman spectrum. The amount of each of the five possible Q^n configurations is used to define the connectivity of the glass structure (Brawer & Wright, 1977; Mysen *et al.* 1982), influenced by the kind and amount of modifiers. A general trend was found for the medieval-like glasses: with the increase of K_2O the quantity of Q^1 and Q^2 configurations increased at the expense of Q^3 and Q^4 configurations (Shelby, 2005; Malfait *et al.,* 2007, 2008), indicative of an increasing de-polymerization.
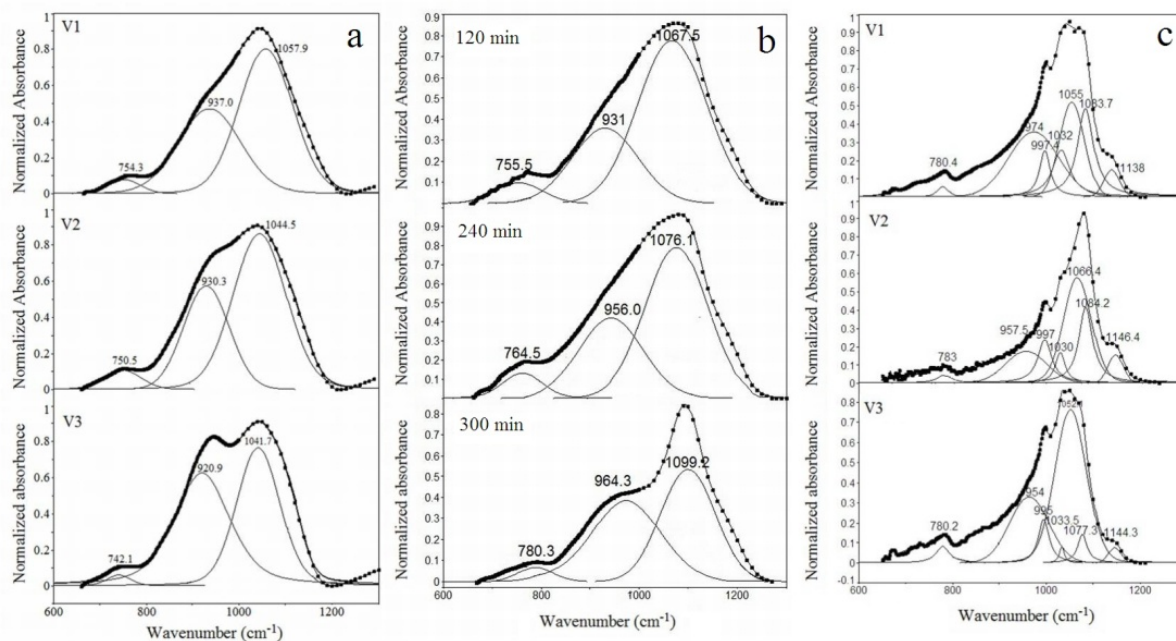
Fig. 1 - a) Fit (thick line) of the unaltered V1, V2 and V3 FT-IR spectra (points) through decomposition (thin lines) into vibrational contributions; b) Fit (thick line) of the leached V3 samples FT-IR spectra (points) through decomposition (thin lines) into vibrational contributions, over the leaching time; c) Fit (thick line) of the V1, V2 and V3 FT-IR spectra (points) through decomposition (thin lines) into vibrational contributions, after dissolution experiments.
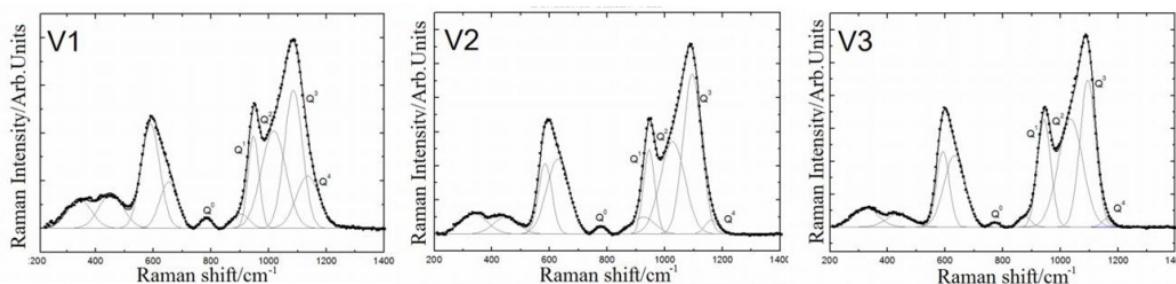

Fig. 2 - Fit (thick line) to the V1, V2 and V3 Raman spectra (points) through de-composition (thin lines) into the Q^n contributions.

δ_{max} and ν_{max} positions

The wavenuber of the bending maximum can be correlated to the glass composition since changes in cations size and charge modify the Si-O-Si angle for geometrical and electrical reasons (Colomban *et al.*, 2006). In silica glass the inter-tetrahedral angle is distributed around l44° (corresponding to a bending peak position of ~ 500 cm^{-1} (Malfait & Halter, 2008)) and a shift toward higher wavenumbers corresponds to a reduction of the angle (Matson *et al.*, 1983, Ziemath & Aegerter, 1994; Malfait *et al.*, 2007, 2008). In the reproduced glass a small wavenumber increase, from ~ 593 cm^{-1} in V1 to ~ 602 cm^{-1} in V3, was observed because of the increased steric effect due to the increased number of modifier cations (Scanu *et al.*, 1994).

The ν_{max} position, corresponding to the Q^3 configurations, depends on the kind of fluxing agent and the values of ~ 1080-1090 cm^{-1} found for the reproduced samples, matches the frequency ranges reported in literature for medieval K- and Ca- rich samples (Colomban *et. al.*, 2006; Colomban & Tournié, 2007; Colomban, 2008; Prinsloo & Colomban, 2008).

Polymerization index I$_p$

The studies carried out on ancient glass evidenced the relationship between the I$_p$ value and: *i)* the kind (defining the different chemical classes) and quantity of flux agents (Colomban, 2008; Prinsloo & Colomban, 2008); *ii)* the glass processing temperature (Colomban, 2003); *iii)* the degree of deterioration of altered surfaces (Colomban & Tournié, 2007). The melting temperature of PLS medieval glass was almost 1350 °C (Eramo, 2006) and would correspond to I$_p$ values higher than 4 (Colomban, 2003); on the contrary these glasses normally give an I$_p$ value < 0.5, suggesting that the annealing, usually performed at temperature of ~ 650-700 °C (Eramo, 2006), was the thermal treatment responsible for the medieval glass polymerization degree. The I$_p$ parameter calculated for the glasses prepared in this study, and annealed at similar temperatures (from 638 °C for V3 to 726 °C for V1) is ~ 0.3-0.4 for the three compositions. In our samples, belonging to the same chemical class (K- modifier) and annealed in a restricted range of temperatures, the I$_p$ cannot significantly differ and this result well matches the data reported in literature.

GLASS AGEING AND CHARACTERIZATION

PLS glass is particularly sensitive to alteration phenomena owing to its high content in network modifiers (Melcher & Schreiner, 2004, 2005), especially potassium, that is weakly bound to the Si-O network because of its low field strength value (Douglas & Isard, 1949; Bunker *et al.*, 1983; Sterpenich & Liburel, 2001), and to the low silica content. Historical window glasses are attacked by atmospheric pollutants conveyed by water in liquid or vapour form (rain, humidity, fog) with the formation of a thin water film which activates the glass alteration process (Hench, 1982; Melcher & Schreiner, 2004, 2005; Sterpenich & Liburel, 2006; Conradt, 2008). In addition, the acid gases present in the atmosphere (CO_2, NO_x, SO_x) dissolve into the deposited water film, lowering its *p*H. For *p*H < 9 the modifiers are extracted from the network through an ion exchange mechanism (leaching) with H^+ or H_3O^+, inducing a hydration process and forming a surface alkali-depleted layer:

$$-Si\text{-}O^-M^+_{(gl)} + H^+_{(aq)} \leftrightarrow -Si\text{-}OH_{(gl)} + M^+_{(aq)} \qquad (1)$$
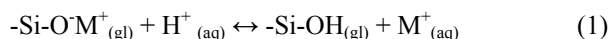
In absence of medium refresh, the alkali and alkaline-earth ions accumulate in the aqueous film, which is depleted in H^+. Dissociated strong bases (M^+ and OH^-) (Melcher & Schreiner, 2005) are thus formed, causing the *p*H increase of the water film and when it reaches the value of about 9, the dissolution of the silica network occurs (Douglas & Isard, 1949): finally, Si-O-Si bonds are broken and silanol groups (Si-OH) are formed (Melcher & Schreiner, 2004, 2005):

$$\ldots\text{-}Si\text{-}O\text{-}Si\text{-}\ldots + OH^- \leftrightarrow \ldots\text{-}Si\text{-}O^- + HO\text{-}Si\text{-}\ldots \qquad (2)$$

Two silanols can then condense and produce H_2O molecules (Hench, 1982; Melcher & Schreiner, 2004, 2005; Sterpenich & Liburel, 2006; Tournié *et al.*, 2008; Conradt, 2008):

$$\ldots\text{-}Si\text{-}OH + HO\text{-}Si\text{-}\ldots \leftrightarrow \ldots\text{-}Si\text{-}O\text{-}Si\text{-}\ldots + H_2O \qquad (3)$$

The final step of the alteration process is the reaction of extracted cations with atmospheric gases (CO_2, NO_x, and SO_x) dissolved in the aqueous film, and the evaporation of water leading to the crystallization of salts (Tournié *et al.*, 2008; Melcher & Schreiner, 2004).

To assess the dependence of structural variations on glass chemistry, ageing experiments were carried out following the procedures set up by Tournié *et al.* (2008). To enable the spectroscopic analysis of the alteration surface layers, the experiments were carried out in severe conditions to accelerate the alteration processes. The ion exchange tests (leaching) were performed by dipping small glass fragments (thickness 1-1.5 mm) in concentrated boiling H_2SO_4 from one to two weeks for V1, to eleven hours for V2 and to six hours for V3

depending on the glass stability. A second set of samples underwent the dissolution process at 300 °C and 80 bars through water-attack in autoclave filled with bi-distilled water. Glass samples were left in autoclave for two (V1 and V2) and one week (V3).

Leaching

The SEM images of V1 and V3 samples indicated a different behavior of the leached glasses: after two weeks exposure, the surface of the K-poorest sample (V1) showed only small isolated pits of 70 μm depth (Fig. 3a). This feature represents the typical morphology of the early stage of the glass alteration process, thus indicating that V1glass is very stable. On the other hand, the K-richest and most de-polymerized glass, V3 (Fig. 3b), appeared very vulnerable, with the leached layer extending from 120 μm -after 60 min exposure to the whole sample thickness (~ 1.5 mm) -after 6 hours exposure. These results confirm that in silicate glasses the leaching effect increases with the quantity of de-polymerizing alkaline ions (Brawer & White, 1977).

The different degree of alteration was also reflected in the different samples weight loss: large for sample V3 (23.6 wt.% after only 6 hours) and very small for V1 (0.6 wt.% after 11 hours), whereas the V2 sample shows an intermediate loss (3.5 wt.% after 11 hours). The weight loss well corresponded to the amounts of K^+ lost during the ion exchange process and detected in the leachant H_2SO_4 solution by Atomic Absorption Spectrometry (AAS). The experiments were carried out up to 11 hours on the V1 and V2 samples, whereas for V3 the attack was concluded after 6 hours, when a whole alteration was obtained.

Concerning the alteration products, elongated crystals were observed by means of secondary electron (SE) images and energy dispersive spectroscopy (EDS) maps indicated the presence of S and Ca. Linear sequences of Raman spectra showed that the intensities of the features of Ca-sulphates tended to increase moving toward the surface layer and the de-composition of the main peak shows the contribution of the three phases gypsum, bassanite and anhydrite.

From a structural point of view the analysis of the Raman spectra evidenced the red shift of the ν_{max} value (Q^3 wavenumber) over the ageing time (Table 2). This was caused by the lengthening of the Si-O bonds due to the interactions of the NBO with the protonic species substituting K^+ during the ion exchange. A red shift was also observed in the δ_{max} value, confirming the relationship with the K-content of the glass; finally an increase of the polymerization index was determined with the leaching time. It was attributed to the release of the less bound components Q^0 and Q^1 together with K^+ during the leaching, and to the condensation of silanols.

Table. 2 - Red-shift of the ν_{max} (cm^{-1}) value for V2 and V3 glass over the leaching time in H_2SO_4

	Leaching time					
	0	60	120	180	240	300
V2 ν_{max}	1094	1080	1077	1075	1075	1073
V3 ν_{max}	1093	1089	1089	1085	1075	1051

The decomposition of the FT-IR spectra collected in the leached layer (Fig. 1b) confirmed that structural modifications occurred since the three main bands were shifted at higher frequencies over the ageing time, suggesting the evolution toward a silica-like structure.

Finally the XRD patterns collected on the altered glass surfaces revealed a shift of the main diffraction maximum toward lower 2θ angles with respect to the unaltered samples, confirming that the depletion of K^+ induces the evolution to a silica-richer structure.

Dissolution

The known high aggressiveness of water was confirmed by comparing the weight loss of the V1 samples after two weeks of ageing in H_2SO_4 and in water: 0.8% and 34.4%, respectively. This high weight loss results from both the release of cations and from the loss of material due to the loss of the glass mechanical properties.

In fact, the alteration layer appeared very fragile and tends to detach in form of flakes, as observed by Back Scattered Electron (BSE) and SE images.

The water pH was measured during the ageing experiments and a marked increase, from about 5 to 8.8, 9.1 and 10.5 was observed for V1, V2 and V3 samples, respectively, because of the exchange of glass alkali ions with water protons. As a result of the pH increase, the dissolution of the silica network occurred with the loss of silicon from the glass surface as determined by the Si-EDS maps.

The SEM observations, moreover, showed cracks often crossing the whole altered layers (Fig. 3c), marked flaking effects and the crystallization of phases with various morphologies (Fig. 3d-f).

The XRD patterns collected on the sample surfaces show the presence of two phyllosilicates: gyrolite and reyerite (Clement & Ribbe, 1973). These phases were also identified by Raman spectroscopy in all the samples and in the totally crystallized V3 layer these phases are found associated to hydroxyapatite and charoite, a Ca-inosilicate.
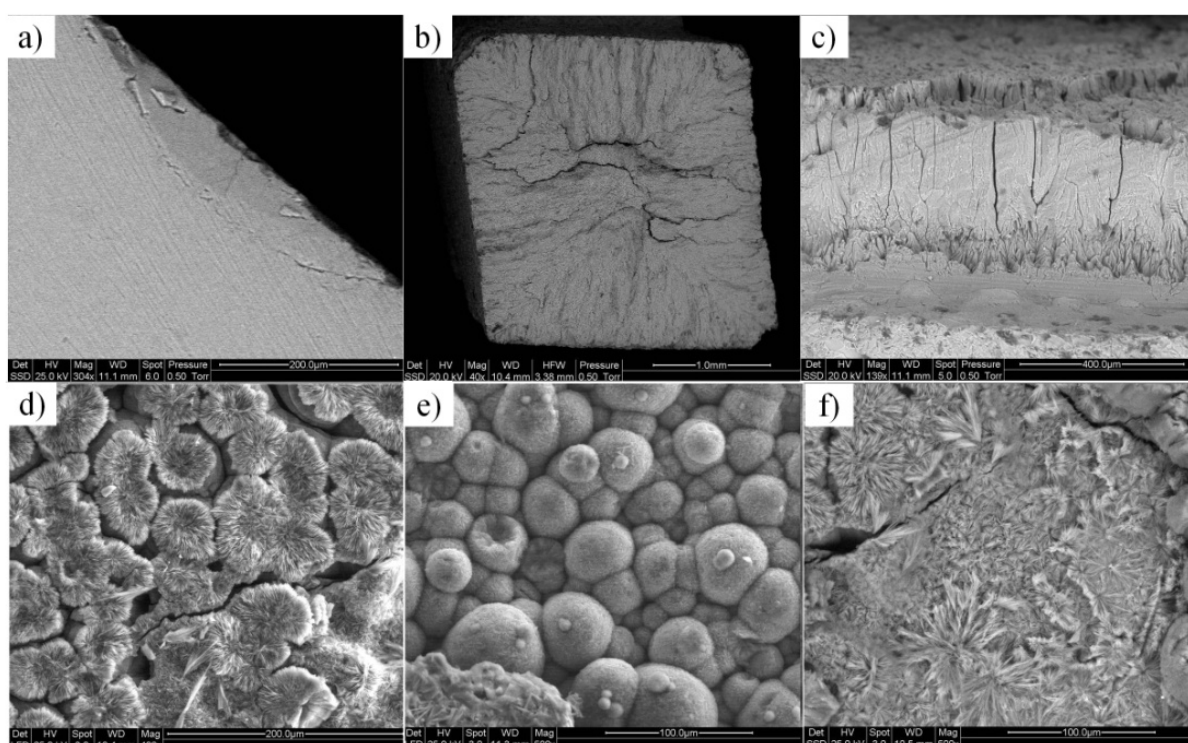

Fig. 3 - a) Backscattered electron (BSE) image of the cross section of a V1 sample aged for 2 weeks in H_2SO_4; b) BSE image of the cross section of a V3 sample aged for 6 hours in H_2SO_4 where the alteration extends to the whole volume; c) BSE image of cracks crossing the alteration layer of the V1 sample after the dissolution experiments; d,f) Seconday Electron (SE) e) BSE images of crystallized phases on the V2 and V3 surfaces.

From a structural point of view, the de-composition analysis carried out on the spectra collected on the V1 and V2 alteration layers showed that the Q^4 units were absent or hardly detectable; moreover also in this case an increase of the I_p parameter, up to 0.8, was found.

The decomposition of the FT-IR spectra (Fig. 1c) displayed the blue-shift of the three main bands and the growth of a shoulder at high frequency. An intensity increase of the main Si-O-Si anti-symmetric stretching band is also observed, accompanied by a decrease of the Si-O⁻K⁺ band intensity. All these spectral changes in the alteration layer are consistent with an evolution toward a structure more similar to that found in silica glass.

SYNTHESIS AND CHARACTERIZATION OF PROTECTIVE COATINGS

From the early 20th century a number of treatments for degraded stained glass panels started, and actually two main approaches exist for their protection: *i)* installation of protective glazings, glass or plastic secondary slabs mounted on the external windows surfaces avoiding, or at least decreasing, the wetting by water in form of rain, fog, moisture, etc. These items, however, reduce the light transmission, inducing the darkening of the glass colors, and have a negative impact on the aesthetic of the monuments; *ii)* application of chemicals for the protection of glass: this method is currently applied only in exceptional cases (Pilz *et al*., 1994). These products must provide good adhesion to the substrate, either corroded or not, and substantially reduce the diffusion of water and pollutants. They must fulfill the requirements of the field of the Conservation of Cultural Heritage regarding the chemical and physical stability, the compatibility with the substrate, the absence of reactions by-products, the absence of color and transparency. The most used product is Paraloid® B72, but also Primal® AC 33, Plexisol® P-550 and Plextol® B 500 are used. However, these organic polymers are considered not suitable for glass protection because of their chemical and physical properties, that are very different from those of the inorganic substrate (Dal Bianco *et al*., 2008) and usually have quite low T_g values (15-40 °C). A glass slab exposed to summer sun can reach surface temperature of about 40-50 °C and these products can soften and lead to the adhesion of dust to the glass surface with its consequent darkening.

Other products currently used are the ORMOCER®'S (Organically Modified Ceramics), a wide family of hybrid sol-gel (Brinker & Sherer, 1990, Kickelbick, 2007) materials whose properties originate from: *i)* the nature and the relative proportions between the inorganic and organic components; *ii)* the conditions of the inorganic poly-condensation reaction; *iii)* the linking reactions leading to the formation of the organic network bound to the SiO_2-based network.

In this work sol-gel water-repellent hybrid coatings were produced starting from Tetra-ethyl-ortho-silicate (TEOS-$Si(OC_2H_5)_4$), to obtain a silica-based matrix compatible with the glass substrate, and functionalized Si-alkoxides, to achieve a definite matrix elasticity and the required surface water repellency. The organically functionalized alkoxides used in different proportions with TEOS are: Octyl-triethoxy-silane (OTES-$CH_3(CH_2)_7Si(OC_2H_5)_3$); Hexadecyl-trimethoxy-silane (EDTMS-$H_3C(CH_2)_{15}Si(OCH_3)_3$), 3-(trimethoxy-silyl)-propyl-methacrylate (MTMS-$H_2C=C(CH_3)CO_2(CH_2)_3Si(OCH_3)_3$), Trimethyl-ethoxy-silane (TMES-$(CH_3)_3Si(OC_2H_5)$) and Methyl-triethoxy-silane (MTES-$CH_3Si(OC_2H_5)_3$). A list of all the tested compositions, where Si-molarity was fixed at 0.5 and the *p*H at 2, using HCl as catalyst, is reported in Table 3.

Table. 3 - Composition list of the sols in term of the amount of the functionalized alkoxides (wt.%). The missing component is always TEOS. The three best compositions are reported in bold.

Sols compositions				
5% EDTMS	**20% OTES**	20% MTMS	60% MTES	10% TMES + 10% OTES
10% EDTMS	30% OTES	60% MTMS	10% MTES + 10% OTES	10% TMES + 20% OTES
20% EDTMS	40% OTES	10% MTMS + 10% OTES	40% MTES + 20% OTES	40% TMES + 20% OTES
5% OTES	**5% EDTMS + 20% OTES**	15% MTMS + 5% EDTMS	20% TEMS	5% TMES + 15% MTES
10% OTES	10% EDTMS + 10% OTES	20% MTES	60% TMES	15% TMES + 45% MTES

The sols were applied by dip-coating technique on laboratory glass slabs and characterized using spectroscopic methods as UV-VIS (Perkin Elmer double ray Lambda 25 UV-VIS spectrophotometer in the spectral range between 300 and 750 nm, using an untreated slab as reference) to test the transparency and

absence of color of the coatings. The FT-IR spectra were collected on the powdered gel and from the ratio between the Si-O-Si anti symmetric stretching (1160 cm^{-1}) and the Si-OH (940 cm^{-1}) stretching bands, the poly-condensation degree was evaluated. With increasing the amount of the organically-functionalized alkoxide, the poly-condensation was favored.

The sol-gel process was followed by Raman spectroscopy that showed how after 10 min of reaction all the molecules underwent the hydrolysis reaction (Matos *et al*., 1992; Marino *et al*., 2005), as proved by the disappearance of the 652 cm^{-1} peak, assigned to the symmetric stretching of the Si-O when Si is bound to all the alkoxide groups (-OR). Moreover the growth of the 250 and 580 cm^{-1} bands, typical of silica glass, and of a peak at 1047 cm^{-1}, due to the Si-O-Si stretching, proved the formation of a silica-based network.

Static and dynamic contact angle measurements were performed to verify the water-repellency of the surfaces. On the basis of the transparency of the films, the contact angles values and the amount of the organic component, maintained as low as possible to achieve the highest compatibility with the substrate, three compositions were selected (bolded in Tab. 3) and applied by dip-coatings on the most alterable V3 glass.

The treated glass was colorimetrically characterized acquiring spectral images by means of a spectrophotometric scanner (Antonioli *et al*., 2004). According to colorimetric standards, a D65 illuminant and a white standard certified by a metrological laboratory were employed for the image acquisition keeping constant the optical geometry (45°/0°). Samples were placed on a white substrate 4 cm high and data were acquired at a scan rate of 1 mm/s, collecting 700 frames. Color values were obtained in the CIEL*a*b* space for every pixel of the image. Mean values and standard deviations of L* (lightness), a* (redness) and b* (yellowness) data from treated and untreated samples were utilized to calculate the average color difference ΔE* (Oleari, 1998; Antonioli *et al*., 2004) defined as:

$$\Delta E^* = (\Delta L^{*2} + \Delta a^{*2} + \Delta b^{*2})^{\frac{1}{2}}$$

The color differences ΔE* between the uncoated glasses and the treated ones always resulted within the experimental error, indicating no significant color changes.

The samples surfaces were also observed by SEM showing very homogeneous coatings with rare cracks, whose amount obviously decrease with increasing the organic fraction.

The coated medieval-like glasses were than submitted to accelerated ageing experiments under UV-light (at a distance of 17 cm from an UV fluorescent lamp GE F20T12- Medium Bipin blacklight blue bulb whose emission spectrum is centered at 375 nm, 20 W power) for two weeks. Another week of ageing was performed using a hard UV lamp (OSRAM HNS G13 OFR emitting in the spectral range 200-280 nm 15 W power). Other samples underwent the exposure to atmosphere saturated with three different concentrations of SO$_2$: 10, 60 and 120 ppm. Glass samples were located in a laboratory dryer whose lower portion was filled with the acid water and left there for one month for every SO$_2$ concentration. Colorimetric and contact angle measurements were performed on the coated samples before and after the exposures: for the UV-aged samples both the L*a*b* parameters and the angle values result unchanged. After the exposures to the SO$_2$-saturated atmosphere the colorimetric coordinates remained unchanged, whereas the contact angles decreased but always remained higher than 90°, the limit assumed for water-repellency (de Gennes, 1985).

In conclusions the studied coatings result definitely suitable to protect historical window glasses exposed to the environmental weathering since, besides the needed water repellency, they match the main requirements of the field of the Conservation of the Cultural Heritage.

REFERENCES

Abo-Naf, S.M., El Batal, F.H., Azooz, M.A. (2002): Characterization of some glasses in the system SiO$_2$, Na$_2$O·RO by infrared spectroscopy. *Mater. Chem. Phys*., **77**, 846-852.

Antonioli, G., Fermi, F., Oleari, C., Reverberi, R. (2004): Spectrophotometric scanner for imaging of paintings and other works of art. *In*: "Proceed. CGIV 2004 - Second European Conference on Color in Graphics, Imaging and Vision", 219-224.

Brawer, S.A. White, W.B., (1977): Raman spectroscopic investigation of the structure of silicate glasses (II). Soda-alkaline earth-alumina ternary and quaternary glasses. *J. Non-Cryst. Solids*, **23**, 261-278.

Brinker, C.J. & Sherer, G.W. (1990): Sol-Gel Science: The Physics and Chemistry of Sol-Gel Processing. Accademic Press, San Diego, California, 912 p.

Bunker, B.C., Arnold, G.W., Beauchamp, E.K., (1983): Mechanisms for alkali leaching in mixed Na-K silicate glasses. *J. Non-Cryst. Solids*, **58**, 295-322.

Clement, S.C. & Ribbe, P.H. (1973): New locality, formula, and proposed structure for reyerite. *Am. Mineral.*, **58**, 517-522.

Colomban, Ph. (2003): Polymerisation Degree and Raman Identification of Ancient Glasses used for Jewellery, Ceramic Enamels and Mosaics. *J. Non-Cryst. Solids*, **323**, 180-187.

Colomban, Ph. (2008): On-site Raman identification and dating of ancient glasses: A review of procedures and tools. *J. Cult. Herit.*, **9**, e55-e60.

Colomban, Ph. & Tournié, A. (2007): On-site Raman identification and dating of ancient/modern stained glasses at the Sainte-Chapelle. Paris. *J. Cult. Herit.*, **8**, 242-256.

Colomban, Ph., Tournié, A., Bellot-Gurlet, L. (2006): Raman identification of glassy silicates used in ceramic, glass and jewellery: a tentative differentiation guide. *J. Raman Spectrosc.*, **37**, 841-852.

Conradt, R. (2008): Chemical Durability of Oxide Glasses in Aqueous Solutions: A Review. *J. Am. Ceram. Soc.*, **91**, 728-735.

Dal Bianco, B., Bertoncello, R., Bouquillon, A., Dran, J.C., Milanese, L., Roehrs, S., Sada, C., Salomon, J., Voltolina, S. (2008): Investigation on sol gel silica coatings for the protection of ancient glass: Interaction with glass surface and protection efficiency. *J. Non-Cryst. Solids*, **354**, 2983-2992.

de Ferri, L., Lorenzi, A., Bersani, D., Lottici, P.P., Simon, G., Vezzalini, G. (2012): Structural and vibrational characterization of medieval like glass samples. *J. Non-Cryst. Solids*, **358**, 814-819.

de Gennes, P.G. (1985): Wetting: statics and dynamics. *Rev. Mod. Phys.*, **57**, 827-863.

Douglas, R.W. & Isard, J.O. (1949): The action of water and of sulfur dioxide on glass surfaces. *J. Soc. Glass Technol.*, **33**, 289-349.

Du, J. & Corrales, L.R. (2006): Compositional dependence of the first sharp diffraction peaks in alkali silicate glasses: A molecular dynamics study. *J. Non-Cryst. Solids*, **352**, 3255-3269.

Eramo, G. (2006): The glass-melting crucibles of Derrière Sairoche (1699-1714 AD, Ct. Bern, Switzerland): a petrological approach. *J. Archaeol. Sci.*, **33**, 440-452.

Göttlicher, J. & Pentighaus, H.J. (1996): Compositional influence on shape and position of the first sharp diffraction peak (FSDP) in silicate and germanate glasses. *Ber. Bunsen-Ges. Phys. Chem.*, **100**, 1563-1568.

Hench, L.L. (1982): Glass surfaces. *J. Phys. Colloques*, **43**, 625-636.

Kickelbick, G. (2007): Hybrid Materials. Synthesis, Characterization, and Applications. G. Kickelbick, ed. Wiley-VCH, Weinheim, Germany, 516 p.

Malfait, W.J. & Halter, W.E. (2008): Structural relaxation in silicate glasses and melts: High-temperature Raman spectroscopy. *Phys. Rev. B*, **77**, 014201-1–014201-6.

Malfait, W.J., Zakaznova-Herzog, V.P., Halter, W.E. (2007): Quantitative Raman spectroscopy: High-temperature speciation of potassium silicate melts. *J. Non-Cryst. Solids*, **353**, 4029-4042.

Malfait, W.J., Zakaznova-Herzog, V.P., Halter, W.E. (2008): Quantitative Raman spectroscopy: speciation of Na-silicate glasses and melts. *Am. Mineral.*, **93**, 1505-1518.

Marino, I.G., Lottici, P.P., Bersani, D., Raschellà, R., Lorenzi, A., Montenero, A. (2005): Micro-Raman monitoring of solvent-free TEOS hydrolysis. *J. Non-Cryst. Solids*, **351**, 495-498.

Matos, M.C., Ilharco, L.M., Almeida, R.M. (1992): The evolution of TEOS to silica gel and glass by vibrational spectroscopy, *J. Non-Cryst. Solids*, **147-148**, 232-237.

Matson, D.W., Sharma, S.K., Philpotts, J.A. (1983): The structure of high-silica alkali-silicate glasses. A Raman spectroscopic investigation. *J. Non-Cryst. Solids*, **58**, 323-352.

Melcher, M. & Schreiner, M. (2004): Statistical evaluation of potash-lime-silica glass weathering. *Anal. Bioanal. Chem.*, **379**, 628-639.

Melcher, M. & Schreiner, M. (2005): Evaluation procedure for leaching studies on naturally weathered potash-lime-silica glasses with medieval composition by scanning electron microscopy. *J. Non Cryst. Solids*, **351**, 1210-1225.

Mukai, A., Kohara, S., Uchino, T. (2007): Modification of medium-range order in silica glass by ball-milling: real-and reciprocal-space structural correlations for the first sharp diffraction peak. *J. Phys. Condens. Matter*, **19**, 455214-1–455214-7.

Mysen, B.O., Virgo, D., Seifert, F.A. (1982): The structure of silicate melts: Implications for chemical and physical properties of natural magma. *Rev. Geophys.*, **20**, 353-383.

Oleari, C. (1998): Misurare il colore. Hoepli Ed., Milano. 442 p.

Pilz, M., Römich, H., Fuchs, D.R. (1994): Protective coatings based on ORMOCER[®] (Stained Glass Windows and Bronze Statues). *In*: "Proceedings of IIC Nordic Group-Danish section, XIII Congress, Surface treatments: cleaning, stabilization and coatings", 193-202.

Prinsloo, L.C. & Colomban, Ph. (2008): Raman spectroscopic study of the Mapungubwe oblates: glass trade beads excavated at an Iron Age archaeological site in South Africa. *J. Raman Spectrosc.*, **39**, 79-90.

Scanu, T., Guglielmi, J., Colomban, Ph. (1994): Ion exchange and hot corrosion of ceramic composites matrices: A vibrational and microstructural study. *Solid St. Ionics*, **70-71**, 109-120.

Schalm, O., Janssens, K., Wouters, H., Caluwé, D. (2007): Composition of 12-18th century window glass in Belgium: Non-figurative windows in secular buildings and stained-glass windows in religious buildings. *Spectrochim. Acta B*, **62**, 663-668.

Schalm, O., De Raedt, I., Caen, J., Janssens, K. (2010): A methodology for the identification of glass panes of different origin in a single stained glass window: Application on two 13th century windows. *J. Cult. Herit.*, **11**, 487-492.

Shelby, J.E. (2005): Introduction to glass science and technology. The Royal Society of Chemistry Ed., Cambridge, 291 p.

Sterpenich, J. & Libourel, G. (2001): Using stained glass windows to understand the durability of toxic waste matrices, *Chem. Geol.*, **174**, 181-193.

Sterpenich, J. & Libourel, G. (2006): Water diffusion in silicate glasses under natural weathering conditions: evidence from buried medieval stained glasses. *J. Non-Cryst. Solids*, **352**, 5446-5451.

Swenson, J. & Böriesson, J. (1998): Intermediate range ordering in a network glass. *J. Non-Cryst. Solids*, **223**, 223-229.

Torres, M.M., Freestone, I.G., Hunt, A., Rehen, T. (2008): Mass-Produced Mullite Crucibles in Medieval Europe: Manufacture and Material Properties. *J. Am. Ceram. Soc.*, **91**, 2071-2074.

Tournié, A., Ricciardi, P., Colomban, Ph. (2008): Glass corrosion mechanism: a multiscale analysis. *Solid St. Ionics*, **179**, 2142-2154.

Ziemath, E.C. & Aegerter, M.A. (1994): Raman and infrared investigations of glass and glass-ceramics with composition $2Na_2O \cdot 1CaO \cdot 3SiO_2$. *J. Mater. Res.*, **9**, 216-225.